Supplemental Information

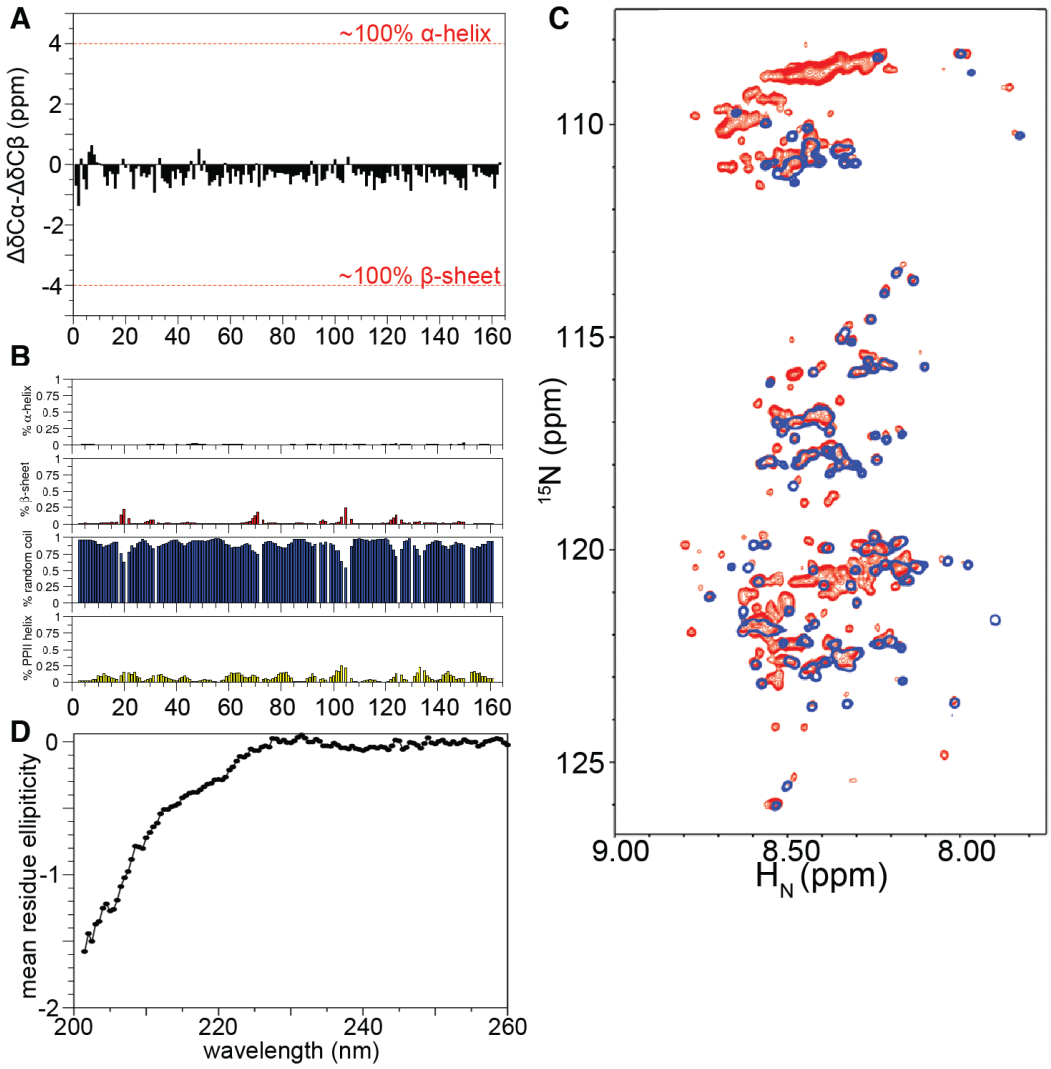

Figure S1. FUS LC is disordered in the dispersed, monomeric state, Related to Figure 1 (**A**) The difference between the observed and predicted random coil Cα and Cβ chemical shift values for FUS LC are between -1 and 1, indicating a disordered protein. (**B**) δ2D predicted secondary structure populations indicate dominant random coil population with minor polyproline II (PPI) and β-sheet population. (**C**) NMR spectrum of backbone amide region (^{1}H-^{15}N HSQC) overlay of FUS LC (blue) and FUS full length (red) demonstrates that FUS LC chemical shifts in FUS full-length protein are globally conserved indicating that the FUS LC domain retains the same disordered structure in the full-length protein. In this figure, 20 μM samples of FUS full length incorporating a C-terminal histidine tag and FUS LC were created by dilution from urea denaturing buffer into 20mM Tris, 2mM DTT, 300 μM $ZnSO_4$, pH 6.5 (**D**) The CD spectrum of the monomeric FUS LC domain.

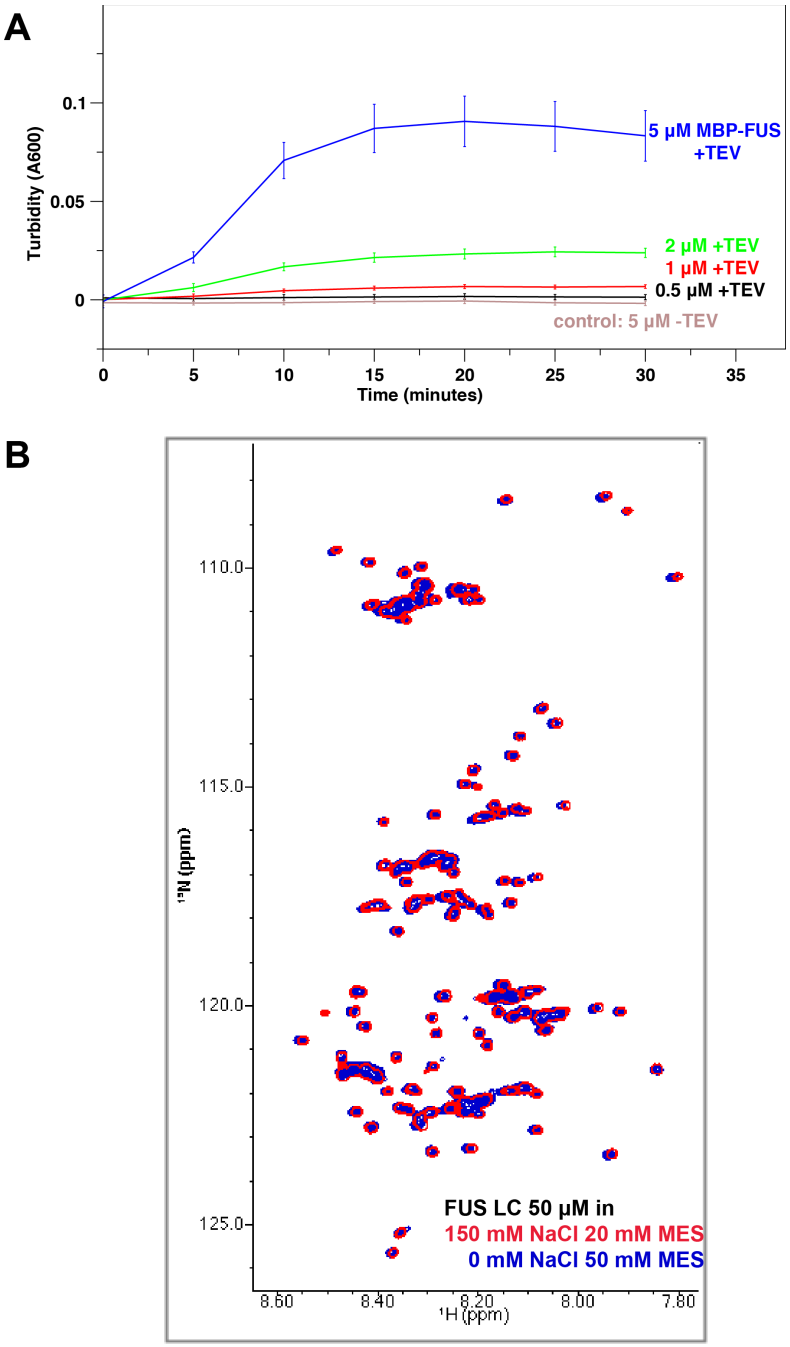

Figure S2. Determinants of phase separation of FUS, Related to Figure 2. (**A**) Extent of phase separation of 50 µl aliquots of increasing concentrations of MBP-FUS with TEV protease. Control (brown) in absence of TEV protease (protease buffer only) at highest concentration of MBP-FUS demonstrates that phase separation requires cleavage and liberation of FUS from the fusion protein. Data are represented as mean +/- st dev of triplicate experiments. (**B**) Structure of FUS LC does not change with increasing NaCl concentration. The ^{1}H-^{15}N HSQC spectrum of FUS LC in 150 mM NaCl 50 mM MES pH 5.5 (red) and 0 mM NaCl 20 mM MES pH 5.5 (blue) are nearly indistinguishable, indicating no changes in global or local structure.

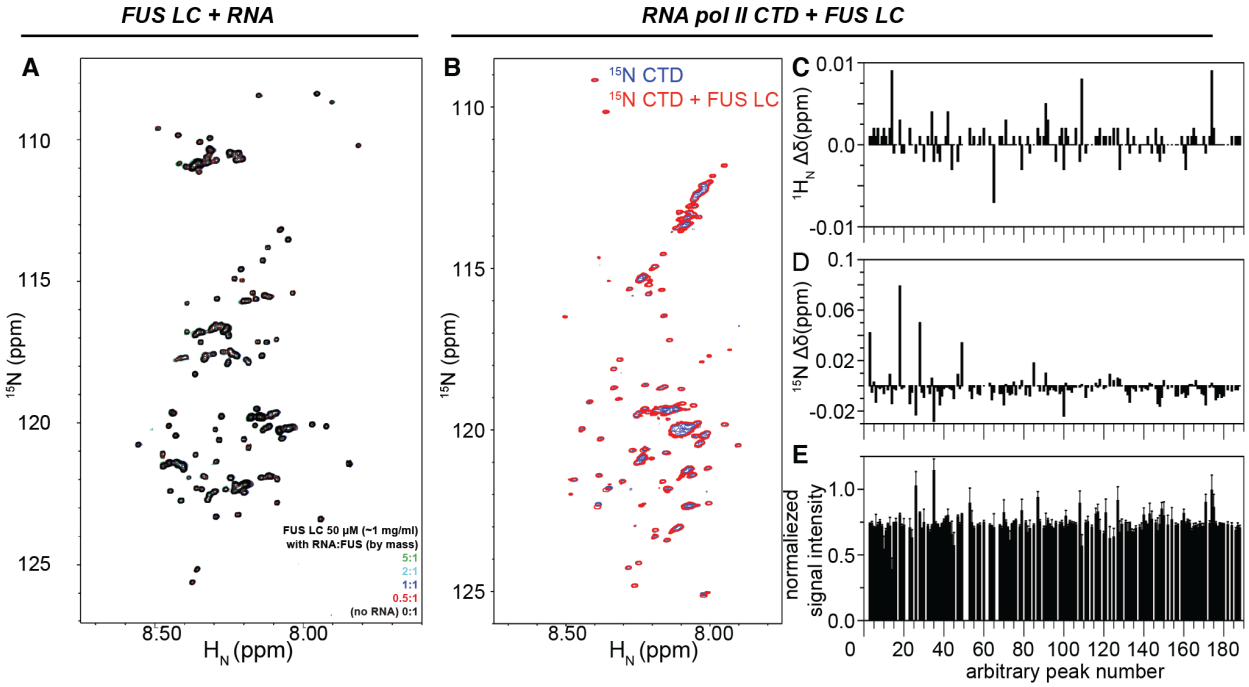

Figure S3. FUS LC and RNA pol II CTD interactions, Related to Figure 3. (**A**) FUS LC does not interact with RNA: NMR spectrum of the backbone amide region (^{1}H-^{15}N HSQC) overlay of the FUS LC with increasing amounts of nonspecific torula yeast RNA demonstrate that there are no significant chemical shifts. **(B-E)** The C-terminal domain of RNA polymerase II (CTD) incorporates into FUS LC droplets. (**B**) NMR spectrum of the backbone amide region (^{1}H-^{15}N HSQC) overlay of the CTD (blue) and equimolar CTD and FUS LC (red) demonstrate that no new resonances are observed. ^{1}H (**C**) and ^{15}N (**D**) chemical shift differences in the CTD and CTD with FUS LC indicate that there is little chemical shift deviation in the resonances in the CTD. (**E**) The decrease in signal intensity to approximately 75% in the CTD with FUS LC relative to the CTD alone. Together these observations suggest that CTD monomers interact primarily with phase separated FUS LC. Note: the peaks of CTD are unassigned and the peak numbers are arbitrarily chosen.

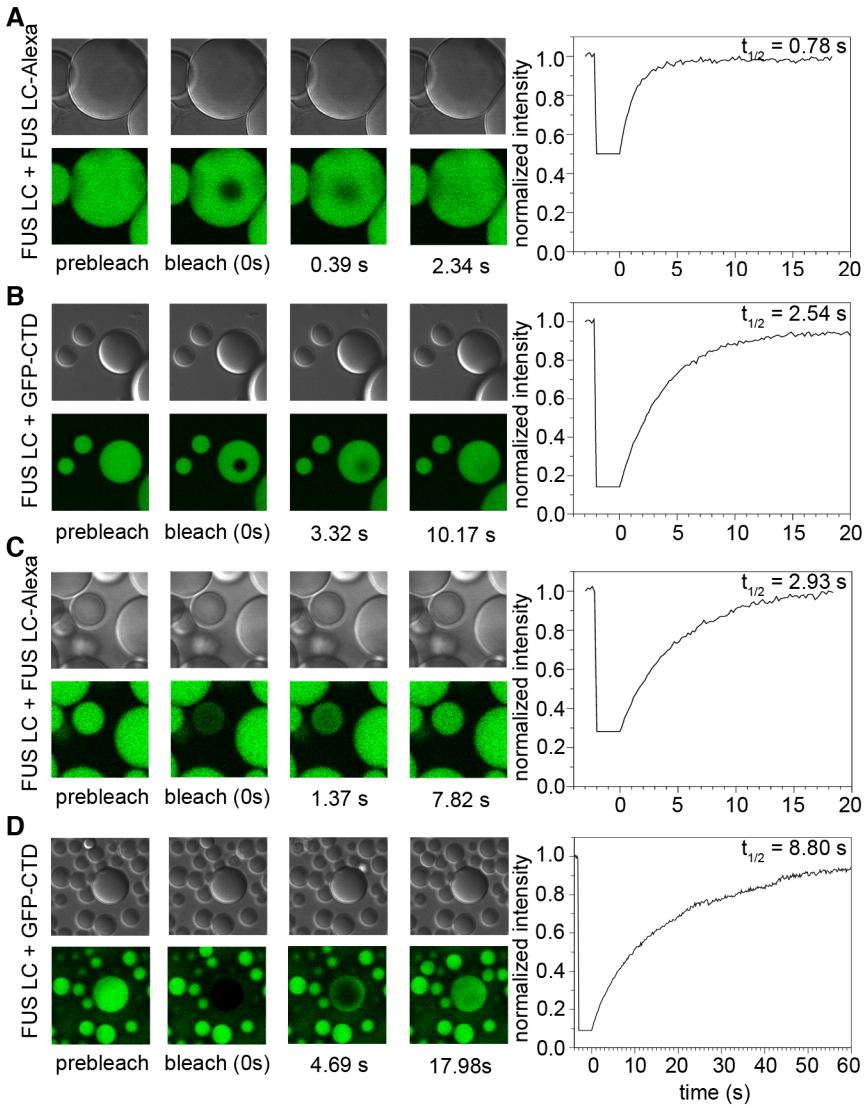

Figure S4. Phase separated FUS LC droplets in low ionic strength buffer show more rapid diffusion and similar turnover as those formed at higher salt concentrations, Related to Figure 4. Example differential interference contrast and fluorescence images (left panels) and FRAP timecourses (right) of partial droplet photobleaching experiments used to measure diffusion constants within the droplets formed in salt-free buffer of FUS LC + FUS LC-Alexa (**A**) and FUS LC + GFP-CTD (**B**). Half times for the selected timecourse are labeled in the recovery curves for 5 μm sized bleach regions. These recovery curves correspond to diffusion constants of 3 and 1 $\mu m^2/s$ for FUS LC and GFP-CTD respectively (see Methods). Example differential interference contrast and fluorescence images (left panels) and FRAP timecourses (right) of full droplet photobleaching experiments used to measure rate of exchange between droplet and dispersed states of FUS LC + FUS LC-Alexa (**C**) and FUS LC + GFP-CTD (**D**). Recovery halftimes were 2.9 ± 0.3 s for ~5 μm FUS LC + FUS LC-Alexa droplets and 10 ± 2 s for ~10 μm GFP-CTD in phase separated FUS LC droplets.

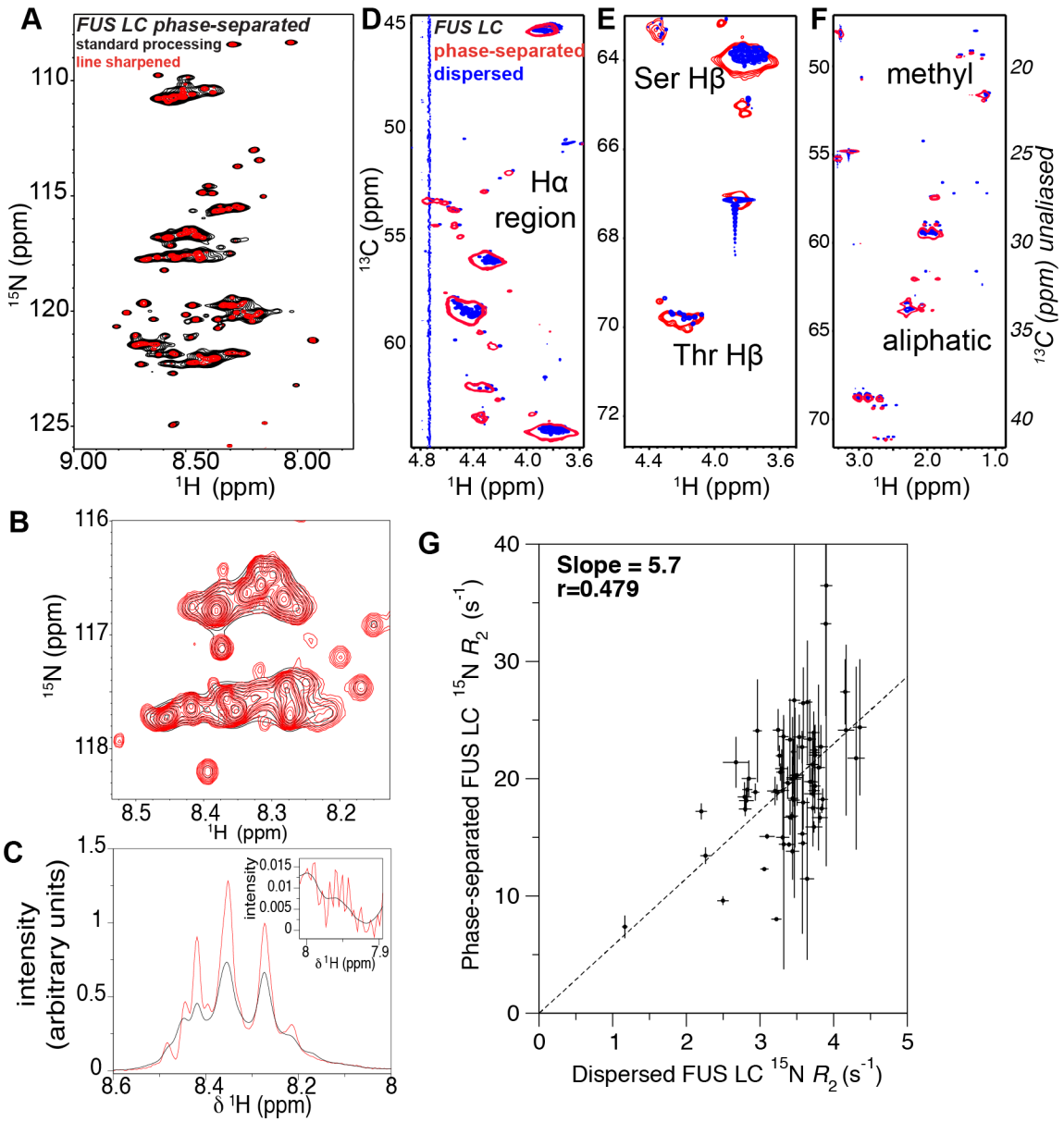

Figure S5. Phase separated FUS LC characterization by NMR. Related to Figure 5. (**A**) Comparison of standard cosine bell (black) and exponential line sharpening (red) processing for FUS LC reveals additional resolved resonances. (**B**) This is evident by zooming to select a representative region of the ^{1}H ^{15}N HSQC where many more resolved peaks are evident in the sharpened processing (red). (**C**) The line sharpening apodization (red) in one dimensional slices through the data (at 117.75 ppm in ^{15}N) provides significant resolution gain over standard processing (black) but at the cost of ~20x lower signal-to-noise (see inset). Note: Data are arbitrarily scaled in intensity axis. Hα, threonine/serine Hβ, and aliphatic/methyl regions (**D**, **E**, **F**, respectively) of ^{1}H ^{13}C HSQC spectra of FUS LC in the phase separated (red) and dispersed (blue) states. Note: ^{13}C resonance positions in (**F**) are aliased, and unaliased ("true") ^{13}C chemical shifts for the methyl and sidechain aliphatic positions in **F** are denoted by italics (right hand side vertical axis ppm labels in **F**). (**G**) Correlation plot comparing ^{15}N R_2 of phase separated and dispersed (monomeric) FUS LC does not show strong correlation.

Supplemental Movie captions

Movie S1. FUS LC phase separation and droplet fusion at water/air interface. Related to Figure 2. Phase separated FUS LC droplets nucleate rapidly at the water/air interface on a glass slide and flow, fuse, and return to spherical shape. Movie is 24 seconds of real time.

Movie S2. FUS LC phase separation and droplet fusion. Related to Figure 2. Adjacent phase separated FUS LC droplets spontaneously fuse and return to spherical shape. Movie is 2 minutes of real time.

Supplemental Experimental Procedures

Section 1: Preparation of samples

Constructs: The following constructs were used for protein expression in BL21 Star (DE3) *E. coli* cultures (Life Technologies):

- FUS LC (residues 1-163, untagged) (modified from gift of Frank Shewmaker, USUHS)
- a FUS LC variant incorporating S86C mutation
- a codon optimized form of the 26 degenerate repeats at the C-terminal domain of DNA-directed RNA polymerase II subunit RPB1 (residues 1773-1790 of the large, catalytic subunit of RNA pol II) (CTD) incorporating a TEV cleavable N-terminal leader sequence and hexahistidine tag (Peti and Page, 2007) synthesized by DNA2.0
- a fusion of GFP followed by the C-terminal domain of RNA polymerase II with 26 heptad repeats (GFP-CTD) which was a gift of Steven McKnight of UT Southwestern
- FUS full length with a C-terminal hexahistidine tag (a gift from Frank Shewmaker, USUHS)
- a fusion of MBP with FUS full length (MBP-FUS, in the pRP1B/THMT vector, gift of Rebecca Page, Brown University).

Expression: Uniformly ^{15}N-labeled FUS LC, CTD, and full length FUS were expressed using M9 media with ^{15}N ammonium chloride as the sole nitrogen source. FUS LC S86C, MBP-FUS, and GFP-CTD were expressed in LB. Cell pellets from 1 liter cultures induced at 0.8 OD600 and harvested after 4 hours at 37 °C were resuspended in 20mM sodium phosphate and 150 sodium chloride pH 7.4 and lysed in an Emulsiflex C3 and the cell lysate was cleared by centrifugation (20,000 g for 60 minutes).

Purification: Soluble MBP-FUS and GFP-CTD were purified using the following protocol. The lysate was filtered with a 0.2 μm syringe filter and loaded onto a HisTrap HP 5ml column. Protein was eluted with a gradient of 0 to 500 mM imidazole in 20mM Tris pH 7.4. Fractions containing MBP-FUS as determined by protein gel were pooled, concentrated and buffer exchanged to 1mM, respectively, into 20mM sodium phosphate pH 7.4 buffer using centrifugal filtration with a 10 kDa cutoff (Amicon, Millipore). GFP-CTD eluted at 11 μM and the elution was used as a stock.

Untagged FUS full length with a C-terminal hexahistidine tag was resolubized in urea and purified as described above in urea containing buffers.

FUS LC variants were resolublized and purified from inclusion bodies in the lysate pellet by the following protocol. The insoluble species were resuspended in 20 mM CAPS pH 11.0 where FUS LC is highly soluble due to protonation of 24 tyrosine residues in analogy to the disaggregation protocols used for amyloid β peptide (Teplow, 2006). The resuspension was cleared by centrifugation (20,000 g for 60 minutes) and the supernatant containing FUS LC was filtered with a 0.2 μm syringe filter. The protein was purified to remove DNA by Q column in 20 mM CAPS pH 11.0 buffers with a gradient of 0 M to 1.0 M NaCl. The protein was then applied to a Superdex 75 26/600 pg column equilibrated with 20mM CAPS pH 11 for further purification. The FUS LC containing fractions were collected and concentrated by centrifugal filtration with a 3kDa cutoff (Amicon, Millipore) to approximately 5-10 mM and flash frozen in aliquots. Purity was confirmed to be >95% by protein gel, ratio of absorbance at 280nm to 260 nm, and two-dimensional NMR.

Section 2: Full-length FUS phase separation assays

To assess the effect of RNA on phase separation, MBP-FUS protein was diluted in 20 mM Tris-HCl 150 mM NaCl pH 7.4 buffer. 2.5 µl of TEV protease stock (0.3 mg/ml in 50 mM Tris-HCl pH 7.5, 1 mM EDTA, 5 mM DTT, 50% glycerol, 0.1% Triton-X-100) or protease buffer was added to create samples with final volumes of 50 µL in 96 well clear plates (Costar®). Torula

yeast RNA was dissolved at 10 mg/ml in 20 mM Tris-HCl 150 mM NaCl pH 7.4 buffer and desalted into the same buffer using a 0.5 ml 7000 MWCO spin desalting column (Zeba, Pierce/ThermoFisher). Desalted RNA was quantified by UV (A260) and then added to samples of 5 μM MBP-FUS (final concentration) in 20 mM Tris-HCl 150 mM NaCl pH 7.4 buffer. Turbidity measurements were recorded at time internals up to 30 minutes after the addition of TEV (or protease buffer for negative control) using a SpectraMax® M5 Microplate Reader (Molecular Devices). Experiments were conducted in triplicate.

To assess the effect of salt on phase separation, MBP-FUS protein was diluted into 20 mM Tris-HCl pH 7.4 buffer with 50, 100, 150, or 300 mM NaCl to a final concentration of 5 μM (0.5 mg/ml using the same approach.

Section 3. Solution NMR samples

FUS LC in the dispersed/monomeric phase samples were created by diluting FUS LC from 20mM CAPS pH 11.0 stock (5 to 10 mM) into 150 mM NaCl 50 mM MES pH 5.5 (pH adjusted with small amounts of BisTris) including 10% $^{2}H_2O$ or 0 mM NaCl 20 mM MES pH 5.5 buffer. Final sample pH was 5.5-5.7. NMR samples of CTD were created using the same procedure. Sample concentrations were estimated using the extinction coefficients calculated by ProtParam (Wilkins et al., 1999).

FUC LC in the phase separated state samples were created as follows. 10 mM stocks of ^{15}N FUS LC in 20mM CAPS pH 11.0 were diluted to 1 mM in 150 mM NaCl 50 mM MES (untitrated, pH 3.5). Samples were 15 ml and were created in standard 15 ml tubes. Samples were heated to 42 °C to clear any initial cloudiness and ensure complete mixing, cooled to room temperature after which a cloudy supernatant above a protein dense phase was already evident. Samples were then quenched on ice to drive further phase separation and centrifuged at 4000 g for 10 minutes at 2 °C. After equilibration at room temperature, a protein-dense liquid phase of ~400 μl was evident at the bottom of the tube. Final sample pH was 5.5. The majority of the supernatant was removed by pipette and the viscous protein-dense phase was transferred to a Shigemi NMR tube by Pasteur pipette. Approximately 300 μl of supernatant was applied on top of the protein-dense phase in place of the usual Shigemi glass insert due to the high sample viscosity. Samples were stable for weeks at room temperature.

Section 4. Solution NMR experiments

All NMR experiments were recorded at 25 °C using Bruker Avance III HD NMR spectrometer operating at 850 MHz ^{1}H frequency equipped with a Bruker TCI z-axis gradient cryogenic probes. Experimental sweep widths and acquisition times (i.e. resolution) and the number of transients were optimized for the necessary resolution, experiment time, and signal-to-noise for each experiment type.

NMR spin relaxation experiments: Motions of the backbone of FUS LC in the dispersed/monomeric phase were probed using ^{15}N R_1, temperature-compensated ^{15}N R_2, and heteronuclear NOE experiments using standard pulse sequences (hsqct1etf3gpsi3d, hsqct2etf3gpsitc3d, hsqcnoef3gpsi, respectively, from Topspin 3.2, Bruker). Interleaved experiments comprised 128*×2048* complex data pairs in the indirect ^{15}N and direct ^{1}H dimensions, respectively, with corresponding acquisition times of 74 ms and 229 ms, sweep width of 20 ppm and 10.5 ppm, centered at 117 ppm and 4.9 ppm, respectively. ^{15}N R_2 experiments had an interscan delay of 2.5 s, a Carr-Purcell-Meiboom-Gill (CPMG) field of 556 Hz, and total R_2 relaxation CMPG loop-lengths of 16.5 ms, 33.1 ms, 82.6 ms, 115.7 ms, 165.3 ms, 181.8 ms, and 264.4 ms. ^{15}N R_1 experiments had an interscan delay of 1.5 s, and total R_1 relaxation loop-lengths of 100 ms, 400 ms, 600 ms, 800 ms, 1.2 s, 1.4 s, and 1.8 s. Heteronuclear NOE experiments were conducted with an interscan delay of 10 s. Data were

processed with nmrPipe(Delaglio et al., 1995), apodized with a cosine squared bell function in the ^{1}H dimension and a cosine bell function in the ^{15}N dimension. Best-fit R_2 relaxation rates were calculated using least squares optimization of $^{1}H/^{15}N$ peak intensities to a single-exponential function.

Motions of the backbone of FUS LC in the phase separated state were measured as described above with the following processing changes: Data were apodized with an *increasing* exponential function (12 Hz and 10 Hz line sharpening in the direct ^{1}H and indirect ^{15}N dimensions, respectively) combined with a cosine squared bell function in the ^{1}H dimension and a cosine bell function in the ^{15}N dimension.

^{15}N single quantum coherence relaxation dispersion experiments were performed with 60 ms R_2 relaxation time with CPMG fields ranging from 50 to 1000 Hz using standard experiments as described previously (Libich et al., 2013).

Assignment experiments: Triple resonance assignment experiments were performed on samples of $^{13}C/^{15}N$ uniformly labeled FUS LC (conditions: 20 mM MES final pH 5.5, 10% $^{2}H_2O$, 25°C). CBCA(CO)NH, HNCACB, HNCO, HN(CA)CO, a high resolution HNCA, and HNN experiments with sweep widths 10 ppm in ^{1}H, 20 ppm in ^{15}N, 6.5 ppm in $^{13}C'$, 56 ppm in ^{13}C for CA/CB experiments and 22 ppm for HNCA using standard Bruker Topspin3.2 pulse programs with default parameter sets. Experiments comprised 42-50*, 128*, 60*, 25*, 2048* complex data pairs in the indirect ^{15}N, indirect $^{13}C\alpha$, indirect $^{13}C\alpha/C\beta$, indirect ^{13}CO, and direct ^{1}H dimensions, respectively. Data were processed with nmrPipe using default linear prediction parameters for either constant time or real time indirect dimensions and assigned in CARA (Keller, 2005).

Assignments of phase separated FUS LC were transferred by overlay from the dispersed/monomeric phase. Sequential assignments were confirmed using ^{1}H ^{15}N HSQC-NOESY-^{1}H ^{15}N HSQC experiments including both remote and directly-attached ^{15}N dimensions ("3D double-^{15}N edited HSQC-NOESY-HSQC") with 50 ms and 150 ms mixing times. Sweep widths were 10 ppm in ^{1}H and 20 ppm in ^{15}N. Experiments comprised 128*, 90*, 2048* complex data pairs in the remote indirect ^{15}N, directly-attached indirect ^{15}N, and direct ^{1}H dimensions, respectively. Data were processed as above and were apodized with an increasing exponential function (4 Hz and 30 Hz in the direct ^{1}H and indirect ^{15}N dimensions, respectively) before application of cosine squared bell function in the ^{1}H dimension and a cosine bell function in the ^{15}N dimensions.

Supplemental References

Delaglio, F., Grzesiek, S., Vuister, G.W., Zhu, G., Pfeifer, J., and Bax, A. (1995). NMRPipe: a multidimensional spectral processing system based on UNIX pipes. J Biomol NMR *6*, 277-293.

Keller, R.L.J. (2005). Optimizing the process of nuclear magnetic resonance spectrum analysis and computer aided resonance assignment. (Zürich, ETH), p. 147 S.

Libich, D.S., Fawzi, N.L., Ying, J., and Clore, G.M. (2013). Probing the transient dark state of substrate binding to GroEL by relaxation-based solution NMR. Proc Natl Acad Sci U S A *110*, 11361-11366.

Peti, W., and Page, R. (2007). Strategies to maximize heterologous protein expression in Escherichia coli with minimal cost. Protein expression and purification *51*, 1-10.

Teplow, D.B. (2006). Preparation of amyloid beta-protein for structural and functional studies. Methods Enzymol *413*, 20-33.

Wilkins, M.R., Gasteiger, E., Bairoch, A., Sanchez, J.C., Williams, K.L., Appel, R.D., and Hochstrasser, D.F. (1999). Protein identification and analysis tools in the ExPASy server. Methods Mol Biol *112*, 531-552.